J Bio Tribo Corros (2016) 2:8
DOI 10.1007/s40735-016-0041-4

Prediction of Removal Rates in Chemical–Mechanical Polishing (CMP) Using Tribocorrosion Modeling

J. Stojadinović[1] · D. Bouvet[2] · S. Mischler[1]

Received: 11 February 2016 / Revised: 15 March 2016 / Accepted: 17 March 2016 / Published online: 4 April 2016

Abstract The influence of electrochemical parameters, open circuit potential, and passivation kinetics, on the removal rates of tungsten in chemical–mechanical polishing (CMP) was investigated in the presented study. Removal rates were measured on a CMP machine, while electrochemical test were performed separately, both using technical CMP slurries. Electrochemical parameters are shown to have a strong influence on tungsten removal rate in CMP. Tungsten removal rate increases with the open circuit potential (electrode potential) and with passivation charge density. A model of Kaufman mechanism previously developed for sliding tribocorrosion of tungsten was adapted to the CMP conditions. This model describes removal rate in terms of both mechanical and electrochemical parameters and was found to effectively rationalize experimental results obtained in different CMP solutions according to their electrochemical properties.

Keywords Chemical–mechanical polishing · Removal rate · Tribocorrosion modeling · Open circuit potential · Passivation charge density

✉ J. Stojadinović
jelenakg@hotmail.com; jelena.stojadinovic@rub.de

[1] Ecole Polytechnique Fédérale de Lausanne, EPFL-TIC, Lausanne, Switzerland

[2] Ecole Polytechnique Fédérale de Lausanne, EPFL-CMI-GE, Lausanne, Switzerland

1 Introduction

Chemical–mechanical polishing is widely used in the production of integrated circuits in order to achieve planar surfaces and remove excess deposited material. The main elements of a CMP system are the wafer with the deposited material to be polished, the pad, and the slurry. The metal to be polished reacts with the oxidants from the slurry by forming a passive film. During polishing, this passive film is abraded by nanoparticles suspended in the slurry and entrained in the contact between the pad and the wafer. The depassivated areas undergo dissolution until the passive film forms again. The cyclic depassivation–repassivation process leads to preferential material removal from the highest loaded asperities and thus to polishing. This phenomenon is known as Kaufmann's mechanism and can be classified as a tribocorrosion process [1–4] involving complex interactions between wear and corrosion.

Preston proposed the empirical Eq. (1) for the calculation of the removal rate RR [5] as a function of pressure between wafer and pad, P, and the linear velocity of the wafer relative to the polishing pad, V. The removal rate is defined as the average thickness change during polishing divided by polishing time:

$$\mathrm{RR} = K_{\mathrm{p}} P V, \tag{1}$$

where K_{p} is the Preston coefficient, varying with process variables such as pad properties, particles size, and slurry composition [6]. Several attempts were proposed to refine Preston equation according to practical experience. Tseng et al. [7] introduced exponents of 5/6 and 0.5 for the pressure and the velocity, respectively. Mpagazehe et al. [8] modeled the fluid dynamics of the slurry and thereof developed hydrodynamic pressure, which is supposed to interfere with the load applied to the contact. Hocheng

et al. [9] provided analytical extension of the Preston equation for dielectrics by including surface charge effect between abrasive particles and SiO_2 surfaces. More recently, Jing Li et al. [10] proposed a theoretical model based on a tribocorrosion approach that describes the total CMP material removal rate as the sum of pure wear, corrosion-induced wear, wear-induced corrosion, and pure corrosion (etching). The model predictions concerning the effect of contact pressure and particle size were found to match experimental results reasonably well. However, none of the proposed models can account for the crucial role played by the chemical composition of the slurries and in particular by their oxidizing power, a key parameter in CMP.

In the present study, we explore another tribocorrosion approach of CMP based on mechanistic models that was found to accurately describe the wear accelerated corrosion of tungsten submitted to sliding in CMP relevant model fluids [1, 4, 11, 12].

Tribocorrosion depends on a multitude of mechanical, material, chemical, and electrochemical factors [13, 14]. A simple view of tribocorrosion was proposed by Uhlig for an inert indenter sliding over a passive metal surface [15]. In this case, two independent mechanisms contribute to material removal from the metal: particle detachment by the indenter digging below the surface (mechanical wear) and accelerated corrosion on the depassivated surface left behind the indenter (wear accelerated corrosion). Both mechanisms are affected by the interaction of mechanical and chemical phenomena. The extent of depassivated area and thus of the wear accelerated corrosion depends on the acting stress field as well as on the resistance and geometrical properties of the contacting materials. On the other hand, the electrochemical conditions established in the contact may significantly affect the mechanical response of metals [11, 16–19]. According to the Kaufmann's model, wear accelerated corrosion is expected to be the determining tribocorrosion mechanisms in CMP.

The tribocorrosion model proposed by Mischler and Landolt [14, 20] (Eq. 2) predicts the theoretical current generated during rubbing, I_{th}, to be proportional to mechanical factors gathered under the parameter R_{dep}, the depassivation rate (the area of bare metal exposed to the solution by unit time), and electrochemical factor Q_p, the passivation charge density (the charge density required to repassivate the metal):

$$I_{th} = R_{dep} Q_p \tag{2}$$

In case of a rough, inert indenter sliding on a soft metal, depassivation occurs at asperity junctions plastically indenting the metal. According to Landolt et al. [14], the depassivation rate for that case can be described by Eq. (3), which predicts a square root dependence of R_{dep} on normal force, provided the number of asperity contacts is independent of normal force.

$$R_{dep} = K_a v_s \left(\frac{F}{H}\right)^{0.5} \tag{3}$$

with $K_a = (k/2)\ \pi^{0.5}\ n_j^{0.5}$, where

- K is the probability factor for an asperity junction to become depassivated,
- n_j is the number of asperity junction established in the contact,
- v_s is the sliding velocity [m/s],
- F is the normal force applied to the contact [N], and
- H is the indentation micro hardness of the metal [Pa].

The goal of this paper is to adapt the above tribocorrosion equations to the CMP situation and to investigate their applicability to a real CMP process. As a model system, CMP of tungsten PVD film deposited on silicon wafer was considered. Polishing was carried out on an industrial CMP device using slurries containing well-defined silica nanoparticles and different oxidizing agents.

2 The Proposed CMP Tribocorrosion Model

In order to establish a transition from the two-body tribocorrosion model (Eqs. 2 and 3) to the CMP tribocorrosion system, the CMP process is depicted here using the schema presented in Fig. 1. On the micro-scale, CMP is characterized by pad asperities in the micrometric range, while wafer asperities are in the nanometric range according to [21]. The normal load on the wafer, F_n, can be expressed

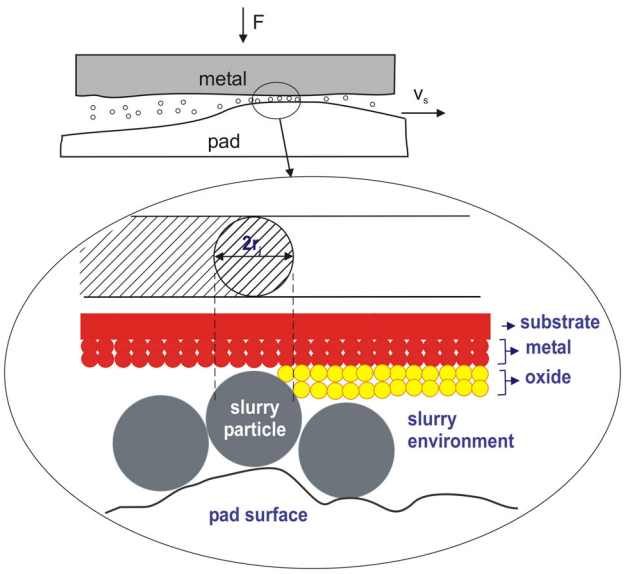

Fig. 1 Schema of the CMP process

using the pressure on the wafer head, P, multiplied by the surface of the wafer on which the metal is uniformly deposited, A_w:

$$F_n = PA_w \tag{4}$$

Relative sliding velocity, v_s, is determined using Eq. (5) knowing the rotation rate of a platen holding the pad, ω_T, and the distance of the centers of the wafer and the pad, r_{cc}:

$$v_s = \omega_T r_{cc}. \tag{5}$$

In the nanometric scale, the removal can be depicted as the particle's scratching action on the surface oxide film. Therefore, instead of considering the number of asperities junctions n_j, we can introduce the number of abrasive silica particles, n_p, acting in the contact. The value of H corresponds to the hardness H_w of the metal deposited onto the wafer that needs to be polished. Equation (6) is a derivation of Eq. (2) by expressing R_{dep}, F_n, and v_s, using Eqs. (3), (4), and (5), respectively, and $K_a = (k/2)\ \pi^{0.5}\ n_p^{0.5}$. Details of the derivation are given elsewhere [14, 20].

$$I_{CMP} = R_{dep}Q = 0.5\pi^{0.5}k\omega_T r_{cc} n_p^{0.5}\left(\frac{PA_w}{H_w}\right)^{0.5} Q \tag{6}$$

The wear accelerated corrosion can be converted into removed volume per unit time V (mm^3/s) using Faraday's law (Eq. 7):

$$V = I_{CMP}\frac{M}{nF\rho}, \tag{7}$$

where M is the atomic mass of the polished metal (g/mol), F is the Faraday's constant (96500 C/mol), n is the valence of dissolution of the metal, and ρ its density (g/cm^3). The CMP removal rate is usually expressed in polished depth by unit time and can be determined using Eq. (8) by considering a uniform removal of the metal on the wafer surface A_w:

$$RR = \frac{V}{A_w} \tag{8}$$

Finally, by combining Eqs. (5)–(8), one obtains Eq. (9), which described the theoretical removal rate expected in CMP:

$$RR = 0.5\pi^{0.5}k\frac{M}{nF\rho}\left(\frac{n_p P}{A_w H_w}\right)^{0.5}\omega_T r_{cc} Q. \tag{9}$$

The present model predicts RR to be a function of the sliding velocity, number of active particles, wafer surface, pressure, wafer hardness, and the passivation charge density, Q. Equation (9) gives a more detailed insight than the Preston equation, although both contain the parameter P and v_s. Note however, that the contact pressure appears at the square root in the present model instead of the linear dependence predicted by Preston equation. A power exponent below 1 was already proposed in past attempts to refine Preston equation [9].

3 Experimental

3.1 Investigated Slurries

The following slurries were investigated:

- slurries containing 3 % silica particles and different contents of KIO_3 (0, 0.1, 2 and 4 %) with pH 5,
- slurries containing 3 % silica particles and different contents of KIO_3 (0, 0.1, 2 and 4 %) with addition of HCl in order to achieve pH 2,
- slurries containing 3 % silica particles, 5 % H_2O_2, different contents of $Fe(NO_3)_3$ (0 %, 0.001 %, 0.02 %, 0.05 %) and HCl in order to adjust the pH. These slurries have pH 2.5, except for 0.02 % $Fe(NO_3)_3$, which has pH 3,
- the reference slurry (RS) containing 3 % silica particles, 2 % KIO_3, H_3PO_4, and $C_3H_6O_3$ with a pH 2.75 (adjusted with NH_4OH).

This technical slurry has been used at the Center of Micro-nanotechnology (EPFL) for tungsten polishing. All slurries contained the same silica particles of 12 nm diameter. All the concentrations are given in weight percent.

3.2 Electrochemical Experiments

Tungsten electrodes were prepared by embedding tungsten rods of 5.3 mm diameter (GoodFellow) in epoxy resin. The flat ends were left free, one was exposed to the solution while the other served for electrical connection. Prior to immersion to the solution, the flat end was polished with grit paper 600, rinsed with alcohol and distilled water, and dried with compressed air.

Open circuit potentials (OCP) for tungsten samples were measured using a mercury sulfate reference electrode and a multimeter. All the potentials in this paper will be given with respect to the mercury sulfate reference electrode, which potential with respect to the standard hydrogen electrode is 0.654 V. The OCP values were measured after 60 s immersion in the investigated slurries.

Passivation kinetics was measured using a Wenking LB 95L Auto Range Laboratory Potentiostat. The potentiostat was controlled by a desktop computer equipped with a National Instruments data acquisition board running under Lab View based software. This set-up allows imposing a potential step (rise time of 2 ms) with simultaneous triggering of the current measurement at a sampling rate of 10 K samples/s. The potential was kept initially at the value of −1 V for 3 s and then switched to the arbitrarily selected

potential of 0.2 V during 1 s, for all chosen slurries. This potential was selected because it lies at least 100 mV above all measured OCPs. Three independent tests were carried out in each slurry in order to check the reproducibility.

3.3 CMP Tests

Polishing of tungsten was carried out using the Mecapol E460, Alpsitec CMP machine in the Center of Micro-nanotechnology (CMI) at the EPFL. Tungsten was deposited on the surface of the wafers to be polished (diameter 101.6 mm or 4″) using CVD (chemical vapor deposition). The CMP process parameters were as follows: wafer pressure (pressure on the head) of 5 psi, platen speed of 50 rpm, head (wafer) speed 60 rpm, back pressure (pressure on the back of the wafer) of 0.15 psi, slurry flow of 100 ml/min and polishing time of 60 s. In terms of global planarization at the wafer scale, film thickness was measured at points across the wafer surface and used to calculate within-wafer-nonuniformity (WIWNU). Most commonly, a 49-point measurement grid is used to determine the WIWNU [22].

4 Results

Open circuit potentials, measured in slurries with different contents of KIO_3 and having different pH, are given in Table 1. When the concentration of KIO_3 reaches 1 %, the saturation occurs and the OCP is stabilizing for both pH values. OCP values are lower for the pH 5 compared to pH 2 values. OCP, measured in slurries containing oxidizing agent H_2O_2 and different contents of $Fe(NO_3)_3$, are also given in Table 1. When the concentration of $Fe(NO_3)_3$ reaches 0.02 %, the saturation occurs and the OCP stabilizes.

The passivation transients in Fig. 2a and b show the increase of current when increasing the concentration of KIO_3. Regarding the passivation transients in Fig. 2c, the clear trend of current increase when increasing the concentration of $Fe(NO_3)_3$ could not be observed. Passivation charge densities measured in technical CMP slurries, Q, are given in Table 1. They were calculated by integrating the measured current [1] (Fig. 2) from the first point acquired after potential change in the potential step experiments (from −1 V up to 0.2 V), corresponding to 0.003 s up to 0.1 s.

The removal rates of tungsten, measured in the technical CMP slurries using the CMP machine, are also given in Table 1.

5 Discussion

5.1 Influence of Electrochemical Parameters on the Removal Rates in Tungsten CMP Practice

5.1.1 Influence of Electrode Potential

Figure 3 shows the influence of OCP of the slurry and its pH on tungsten removal rates. For the same slurry

Table 1 Composition of technical CMP slurries, pH, OCP, Q and CMP removal rates (RR)

Slurry composition		pH	OCP (mV)	Q (μC/mm^2)	RR (Å/min)
3 % silica part.	0.0 % KIO_3	5	−662 ± 15	1 ± 0	40
	0.1 % KIO_3		−406 ± 3	4 ± 0	140
	0.5 % KIO_3		−356 ± 5	10 ± 2	750
	2.0 % KIO_3		−322 ± 7	25 ± 0	1500
	4.0 % KIO_3		−323 ± 8	33 ± 1	1600
3 % silica part.	0.0 % KIO_3	2	−554 ± 11	12 ± 1	25
HCl	0.1 % KIO_3		−121 ± 11	11 ± 1	200
	0.5 % KIO_3		−75 ± 9	15 ± 0	1150
	2.0 % KIO_3		−30 ± 9	20 ± 3	1950
	4.0 % KIO_3		−54 ± 8	25 ± 3	NA
"RS"					
3 % silica part.					
H_3PO_4	2.0 % KIO_3	2.75	−150 ± 9	38 ± 2	2300
$C_3H_6O_3$					
NH_4OH					
3 % silica part.	0.0 % $Fe(NO_3)_3$	2.5	−296 ± 6	>7 ± 0	300
5 % H_2O_2	0.001 % $Fe(NO_3)_3$	2.5	−85 ± 3	>7 ± 0	NA
HCl	0.02 % $Fe(NO_3)_3$	3.0	64 ± 7	>4 ± 0	1670
	0.05 % $Fe(NO_3)_3$	2.5	79 ± 9	>9 ± 1	2270

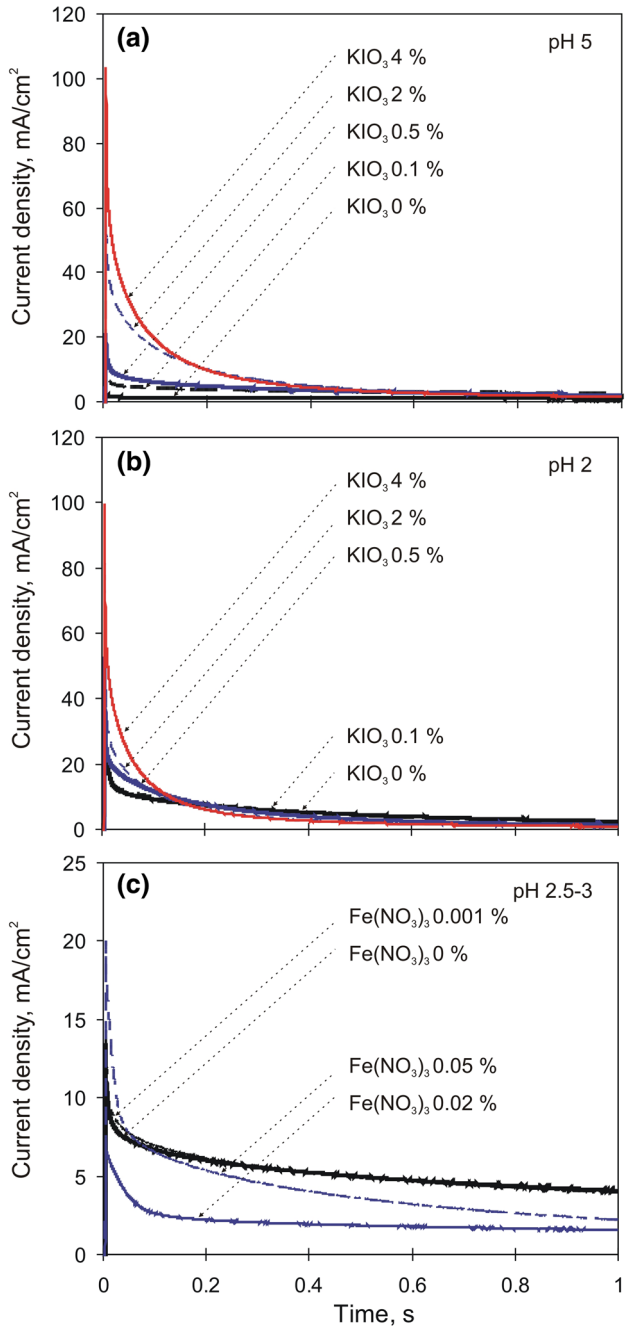

Fig. 2 Passivation transients for the slurries with different concentrations of the oxidizing agent: **a** KIO_3 (pH 5), **b** KIO_3 (pH 2) and **c** $Fe(NO_3)_3$ (pH 2.5–3)

composition (KIO_3 slurries), both OCP and removal rates have higher values for pH 2 than for pH 5.

The same trend, higher the OCP, higher the removal rate, is observed for the slurry containing H_2O_2 and different concentrations of $Fe(NO_3)_3$. The reference slurry RS is also presented in Fig. 3. High values of removal rates in the case of the RS slurry are probably more related to different chemistry than to its OCP value.

The OCP shift to higher values, when decreasing pH from 5 to 2 in the presence of KIO_3 (Table 1; Fig. 3), can be explained using the Pourbaix diagram for tungsten [23]. Tungsten passivation behavior is discussed elsewhere [12]. In order to calculate the shift of potential due to pH change from 5 to 2, the reaction (3) is used. Nernst equation for tungsten oxidation ($W + 3H_2O \rightarrow WO_3 + 6H^+ + 6e^-$) at 25 °C can be written as follows:

$$E_{rev} = -0.119 - 0.059\text{pH} \quad (10)$$

The equilibrium potential calculated using the Eq. (10) for pH 2 is equal to −0.895 V MSE and for pH 5 is equal to −1.072 V MSE. The pH decrease from 5 to 2 should cause the potential change of 180 mV. This is in agreement with the test results shown in Fig. 3, and can be explained with the fact that the oxidation of tungsten for pH 5 starts at lower potentials compared to pH 2, as suggested in Pourbaix diagram for tungsten [23]. The reason for the significant increase of tungsten removal rate for both pH 2 and pH 5 (Fig. 3) beyond the certain potential value is not clear. For pH 2, this threshold potential value (−0.1 V) belongs to the passive region, where WO_3 is already formed, according to Pourbaix diagram [23]. For pH 5 at the potential value of -0.4 V MSE, which is marking significant change of removal rate, only metallic tungsten should be found at the surface.

5.2 Influence of Passivation Charge Density

In analogy with OCP influence, also the passivation charge density increase leads to the increase of the removal rate for both groups of KIO_3 slurries (pH 2 and 5), as shown in Fig. 4. Reference slurry, RS, shows the highest removal rate and the highest passivation charge density. It is necessary to pay attention that removal rates obtained on the

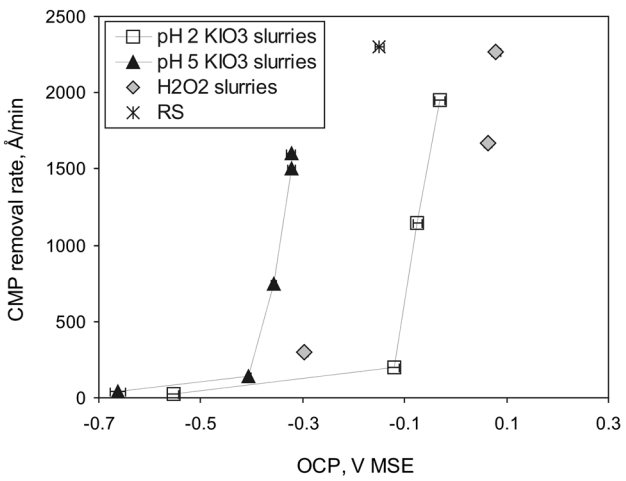

Fig. 3 Influence of the OCP and pH on the CMP removal rate

CMP machine relate to the OCP values of slurries, but no potential was imposed on the CMP machine during polishing. The calculated passivation charge (Table 1) relates to the same fixed imposed electrode potential for all the slurries (0.2 V MSE). Measured passive current (Fig. 2) for all technical slurries (Table 1) is probably highly influenced by the cathodic reaction. According to Pourbaix diagram for I [23], the reaction occurring in the presence of KIO_3 slurries is the following one:

$$I_2 + 6H_2O = 2IO_3^- + 12H^+ + 10e^- \quad (11)$$

The E_{rev} values for this reaction are equal to 0.38 V MSE and 0.16 V MSE for pH 2 and pH 5, respectively, according to the equation:

$$E_{rev} = 1.178 - 0.0709\,pH + 0.0059\log\frac{(IO_3^-)}{(I_2)} \quad (12)$$

As presented in Fig. 5, the measured current represents the sum of the anodic and the cathodic current. The test potential for passivation kinetics measurements was 0.2 V. The influence of the excess cathodic current (reduction of *I*) cannot be neglected for pH 2. For a simple electrode, it is schematically shown in Fig. 5. On the other hand, for pH 5, at the potential of 0.2 V, the contribution of the anodic current is more important.

The effect of the important contribution of the cathodic current to the overall current measured during passivation kinetics measurement is also present in the slurries containing H_2O_2. Therefore, the calculated $Q_{p_{CMP}}$ values for these slurries (Table 1) are underestimated.

Hydrogen peroxide is unstable and reducible to water below 0.93 V MSE and unstable and oxidizable to oxygen above the potential of −0.09 V MSE [23]. These two domains of instability have a common area in which hydrogen peroxide is doubly unstable and can decompose into water and oxygen according to reaction (6):

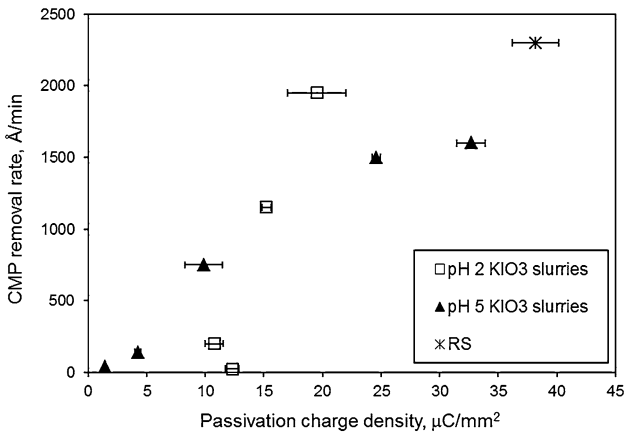

Fig. 4 Influence of the passivation charge density on the CMP removal rate

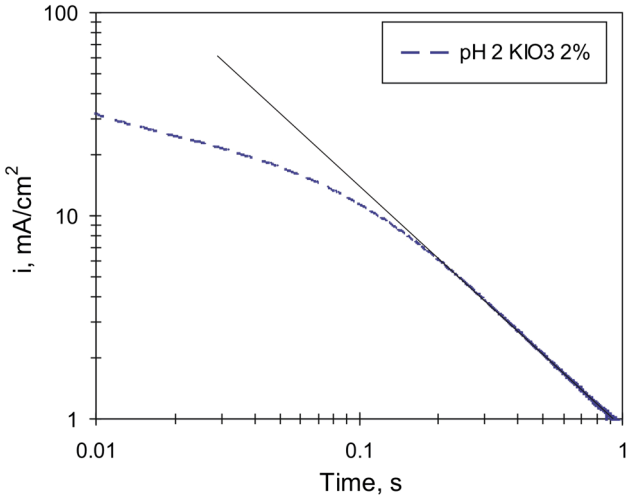

Fig. 5 Influence of cathodic partial reaction on the resulting current regarding the passivation kinetics measurements undertaken at 0.2 V

$$2H_2O_2 \rightarrow 2H_2O + O_2 \quad (13)$$

In the performed potential step experiments, the imposed electrode potential was 0.2 V MSE that is situated in the hydrogen peroxide double instability region.

A way to refine the measurements of passivation kinetics should be to take into account the OCP value of the given slurry and to impose the potential corresponding to the OCP of the given slurry augmented by 200 mV.

Despite the simplifications made in the passivation kinetics measurements, related to imposing the fixed potential of 0.2 V after the potential change, the influence of passivation kinetics on the removal rate is clear, as shown in Fig. 4.

The influence of KIO_3 concentration on the CMP removal rate and OCP is shown in Fig. 6a, b. When increasing the KIO_3 concentration, saturation of CMP RR and OCP occurs for both pH 2 and pH 5.

5.3 Quantitative Prediction of the Removal Rate in CMP Using Tribocorrosion Model

In order to predict the RR using the Eq. (9) it is necessary to correctly determine the passivation charge density, which is a complex issue. One of the methods would be to integrate the values of current measured in potential step experiments [1]:

$$Q = \int_o^{t_d} i_{ex}\mathrm{d}t \quad (14)$$

The typical passivation transient for technical slurry containing 2 % KIO_3 for pH 2 is shown in Fig. 7. The current in the initial period is limited by the ohmic resistance of the solution. Therefore, the current can be

extrapolated from the linear passivation region, for the time value of 0.003 s, which corresponds to the first acquired value after the potential change in potential step experiments. The extrapolation equation used for the technical slurry 2 % KIO_3 at pH 2 is given with Eq. (15):

$$i_{ex} = 1.02 \cdot t^{-1.1} \quad (15)$$

The integration period, t_d, is defined as a time interval between two particles' depassivation actions at the same wafer area. It can be calculated using the Eq. (16), where l_p is a distance between a particle depassivating the wafer surface and the subsequent one coming into the contact. Since the pad asperities are not taken into account, determination of the distance between two particles (one in depassivation action and the following one) and of the time interval, t_d, remains approximate.

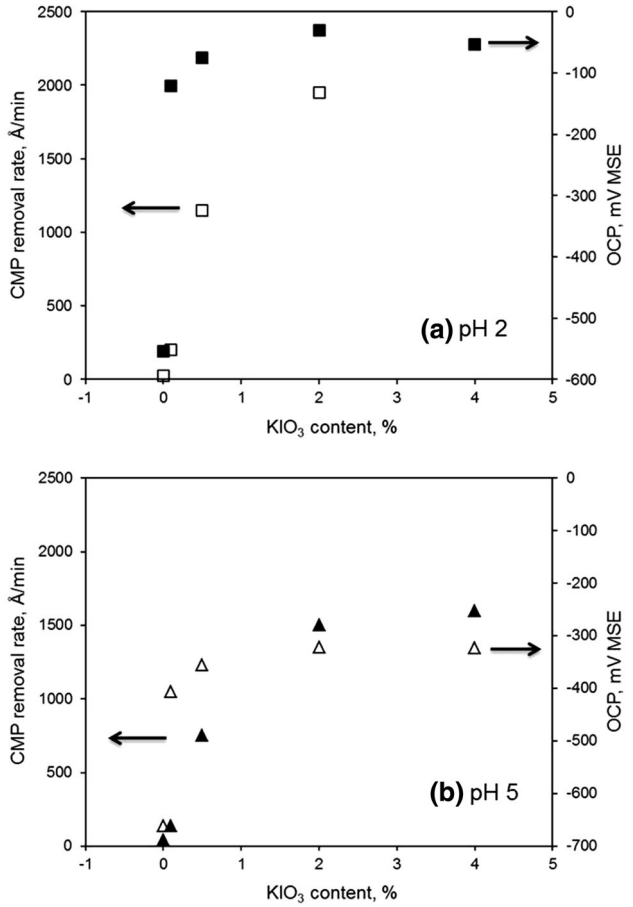

Fig. 6 Influence of KIO_3 concentration on the CMP removal rate and OCP for: **a** pH 2 and **b** pH 5

The number of particles in contact effectively depassivating the wafer surface, n_p, is dependent on several factors. Firstly, n_p, is proportional to the number of particles present in a solution. Further on, it depends on a separation distance, $d_{sep} = f(F, v_s, r_p)$, between the wafer and the pad during polishing under pressure [24]. Some of the particles present in solution can be embedded in the pad [25], while others are captured by asperities [26]. Besides the sliding motion, also the rolling takes place for certain number of particles in contact with wafer, and possibly contributes the depassivation of the surface [27]. Due to these effects, the evaluation of the n_p is complex. Nevertheless, the number of particles in contact effectively depassivating the wafer surface can be estimated using the Eq. (17).

$$t_d = \frac{l_p}{v_s} = \frac{\left(\frac{A_w}{n_p}\right)^{0.5}}{v_s} \quad (16)$$

$$n_p = \frac{f_p A_w}{r_p^2 \pi} \quad (17)$$

Fractional surface coverage of particles embedded on the pad and wafer, f_p, was found to vary with particle size, load, and particle concentration from values below 0.1 up to 0.8 [25]. In the absence of valid data for the present slurry composition, full coverage of particles was assumed leading to $f_p = 1$. The movement type ratio slide/roll of the particles was not taken into account in the n_p determination for the quantitative prediction of the RR. The same hold for particles buried in the pad or trapped in surface depressions.

Pad diameter is equal to 558.8 mm (22″) and the value of r_{cc} is taken as constant (140 mm). Normal load in the CMP can be calculated using the pressure on the wafer head, P, equal to 5 psi (34.5 kPa). The value of the tungsten wafer surface (CVD layer) hardness, H_{CMP}, during the CMP process

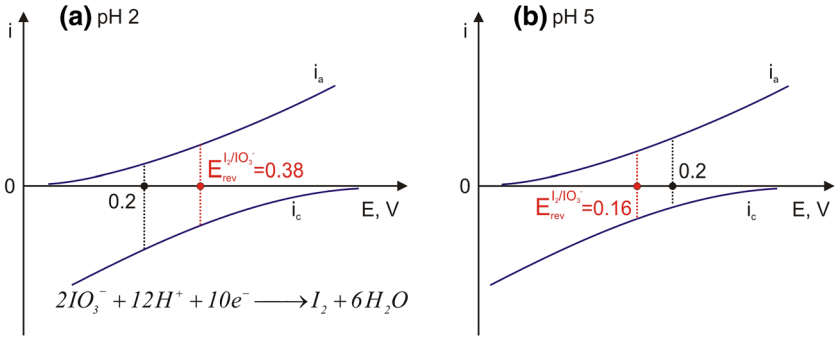

Fig. 7 Extrapolated current density from passivation kinetics measurements

is not known, but we can approximately assume it has equal value to the hardness of tungsten samples (3.7 GPa).

The calculated passivation charge density for the time period t_d in the slurry containing 2 % KIO_3 for pH 2 equals 3.1 10^{-7} mC/mm^2.

Taking into account the above explained parameters, the maximum calculated RR has the value of approx. 30,000 Å/min for tungsten during polishing in the slurry containing 2 % KIO_3 at pH 2. The *RR* calculated using the explained model is one order of magnitude higher than RR measured on the CMP machine in the same technical slurry (Table 1). This discrepancy is most likely due to the assumption of full particle coverage f_p that is expected to overestimate the number of active, depassivating particles and thus the removal rate. Clearly, improved quantification of this factor is a prerequisite for further developing the quantitative predictability of the present tribocorrosion model.

6 Conclusions

- Electrochemical parameters (OCP, passivation charge density) are strongly influencing tungsten CMP removal rate (RR). Tungsten removal rate increases when increasing the value of these electrochemical parameters. Under given CMP polishing conditions (known OCP and passivation kinetics), it would be possible to rationalize the industrial CMP outcome based on the developed scientific criteria.
- The simplified method used for determination of the passivation charge density does not diminish the clarity of the observed increasing trend of tungsten CMP removal rate and tribocorrosion wear rate with passivation charge density.
- The tribocorrosion model can be successfully applied to tungsten CMP practice. The results of the undertaken study are in a good agreement with Mischler's model. The assumption is made that the number of asperities in tribocorrosion contact corresponds to the number of abrasive particles in the CMP slurry contributing to the depassivation of tungsten wafer's surface. The advantage of the used tribocorrosion model over the Preston's model is that it allows to semi-quantitatively predict the effect of (electro)-chemical and material parameters (such as the passivation charge) on tungsten removal in CMP, with a reasonable approximation.

References

1. Stojadinović J, Bouvet D, Declercq M, Mischler S (2009) Effect of electrode potential on the tribocorrosion of tungsten. Tribol Int 42(4):575–583
2. Mischler S (2008) Triboelectrochemical techniques and interpretation methods in tribocorrosion: a comparative evaluation. Tribol Int 41:573–583
3. Ziomek-Moroz M, Miller A, Hawk J, Cadien K, Li DY (2003) An overview of corrosion–wear interaction for planarizing metallic thin films. Wear 255:869–874
4. Bielmann M, Mahajan U, Sigh R, Agarwal P, Mischler S, Rosset E, Landolt D (2000) Tribological experiments applied to tungsten chemical mechanical polishing. Mat Res Soc Symp Proc 566:97
5. Preston FW (1927) The theory and design of glass plate polishing machines. J Soc Glass Technol. 11:247–256
6. Steigerwald JM, Murarka SP, Gutmann RJ (1997) Chemical mechanical planarization of microelectronic materials. Wiley, New York
7. Tseng WT, Wang YL (1997) Re-examination of pressure and speed dependences of removal rate during chemical–mechanical polishing processes. J Electrochem Soc 144(2):L15–L17
8. Mpagazehe JN, Higgs CF III (2013) A three-dimensional transient model to predict interfacial phenomena during chemical mechanical polishing using computational fluid dynamics. Proc Inst Mech Eng Part J 227(7):777–786
9. Hocheng H, Tsai HY, Su YT (2001) Modeling and experimental analysis of the material removal rate in the chemical mechanical planarization of dielectric films and bare silicon wafers. J Electrochem Soc 148(10):G581–G586
10. Li J, Lu X, He Y, Luo J (2011) Modeling the chemical–mechanical synergy during copper CMP. J Electrochem Soc 158(2): H197–H202
11. Stojadinović J, Mendia L, Bouvet D, Declercq M, Mischler S (2009) Electrochemically controlled wear transitions in the tribocorrosion of ruthenium. Wear 267:186–194
12. Stojadinović J, Bouvet D, Declercq M, Mischler S (2011) Influence of chelating agents on the tribocorrosion of tungsten in sulphuric acid solution. Electrochim Acta 56:7131–7140
13. Landolt D (2007) Corrosion and Surface Chemistry of Metals, Lausanne, EPFL Press, distributed by CRC Press
14. Landolt D, Mischler S, Stemp M (2001) Electrochemical methods in tribocorrosion: a critical appraisal. Electrochim Acta 46:3913–3929
15. Uhlig HH (1948) Corrosion handbook. John, New York
16. Favero M, Stadelmann P, Mischler S (2006) Effect of the applied potential of the near surface microstructure of a 316L steel submitted to tribocorrosion in sulfuric acid. J Phys D 39:3175–3183
17. Bidiville A, Favero M, Stadelmann P, Mischler S (2007) Effect of surface chemistry on the mechanical response of metals in sliding tribocorrosion systems. Wear 263:207–217
18. Perret J, Boehm-Courjault E, Cantoni M, Mischler S, Beaudouin A, Chity W, Vernot JP (2010) EBSD, SEM and FIB characterisation of subsurface deformation during tribocorrosion of stainless steel in sulphuric acid. Wear 269:383–393
19. Akonko SB, Li DY, Ziomek-Moroz M, Hawk J, Miller A, Cadien K (2005) Effects of $K_3[Fe(CN)_6]$ slurry's pH value and applied potential on tungsten removal rate for chemical–mechanical planarization application. Wear 259:1299–1307
20. Mischler S, Debaud S, Landolt D (1998) Wear-accelerated corrosion of passive metals in tribo-corrosion systems. J Electrochem Soc 145(3):750–758
21. Zantye PB, Kumar A, Sikder AK (2004) Chemical mechanical planarization for micro electronics applications. Mater Sci Eng R 45:89–220
22. Yeruva SB (2005) PhD Thesis Particle scale modeling of material removal and surface roughness in chemical mechanical polishing. University of Florida
23. Pourbaix M (1974) Atlas of electrochemical equilibria in aqueous solutions. National Association of Corrosion Engineers, Houston

24. Jeng YR, Huang PY, Pan WC (2003) Tribological analysis of. CMP with partial asperity contact. J Electrochem Soc 150(10): G630–G637
25. Choi W, Lee SM, Abiade J, Sing RK (2004) Estimation of fractional surface coverage during oxide chemical mechanical polishing (CMP). J Electrochem Soc 151(5):G367–G372
26. Luo J, Dornfeld D (2001) Material removal mechanism in chemical mechanical polishing: theory and modelling. IEEE Trans Semicond Manuf 14(2):112–133
27. Sun D, Wharton JA, Wood RJK, Ma L, Rainforth WM (2009) Microabrasion–corrosion of cast CoCrMo alloy in simulated body fluids. Tribol Int 42(1):99–110